© NOV 2025 | IRE Journals | Volume 9 Issue 5 | ISSN: 2456-8880
DOI: https://doi.org/10.64388/IREV9I5-1722675

Microstructural and Optical Properties of Undoped and Co Doped Zinc Oxide Nanoparticles Via Co-Precipitation Technique

AKANKSHA C JAWLE
Department of Physics, Kai. Rasika Mahavidyalaya, Deoni. Dist. Latur.

Abstract- In this study, we report on the microstructural and optical properties based on Co-doped Zinc Oxide (ZnO) nanoparticles synthesized via co-precipitation technique. All samples were characterized by using x-ray diffraction (XRD) and uv-visible (UV) spectroscopy. Pure and Co-doped ZnO are polycrystalline and well crystalized in the hexagonal crystal structure. XRD results revealed that the lattice constants were decreased with increasing Co doping. Furthermore, cell volume of ZnO sample was reducing after Co-doping. The average crystallite size was found to be decrease from 13.14 nm to 10.07 nm. UV-Visible spectroscopy was used to evaluate the energy band gap of prepared samples and found to decrease with Co-doping. The reported structural and optical properties indicate the potential application of Co-doped ZnO material for opto-electronics application.

***Keywords:** metal oxides; zno; nanoparticles; microstructural properties; energy band gap; opto-electronics.*

I. INTRODUCTION

Optoelectronics devices are incessantly expanding their roles in emerging sciences and technologies that evolve into new industries. In recent decades, advanced technologies in electronics have shown rapid growth, particularly in production of vehicles and telecommunication industries [1, 2]. The entirely new concept of optoelectronics devices at the nanoscale level is rapidly becoming the focus of intense interest and is being intensively investigated globally. The size reduction from microscope to nanoscale rapidly increases the active surface area of materials device and hence the superior the performance. Nanostructures often have a higher surface-to-volume ratio which can increase their efficiency of the device [3 - 5]. Also, the dimensional have found to be an impact on the material property behaviour of the nanostructured based optoelectronics devices. Therefore, zero-dimensional (0D) nanostructures such as nanoparticles have been used for the optoelectronics applications due to high surface area to volume ratio.

The various metal oxide based nanoparticles such as SnO_2, In_2O_3, TiO_2 and CuO have been studied [6 - 8]. Among these, ZnO nanostructures have been widely employed as different device applications because of low cost, simple fabrication, outstanding chemical stability and non-toxicity [9 - 11]. Furthermore, ZnO material exhibited n-type conductivity, wide band gap, high exciton binding energy (60 meV), and strong electron mobility [12]. During the last decades, the number of industries using optoelectronics device has increased largely. In fact, there has been a significant enhance in the interest in developing device which should present key factors. To develop optoelectronics device based ZnO material with superior performance using doping materials via suitable metals [13].

The present study, we selected cobalt as a dopant of ZnO to improve the optical properties of optoelectronics device. Cobalt is cheap and non-toxic to human health other than elements. A co-precipitation method was used to synthesize undoped and Co-doped ZnO nanopowders. The effect of Co doping on the structural property of ZnO were investigated in details.

II. EXPERIMENTS SECTION

A co-precipitation method was used in the fabrication of metal oxides nanoparticles due to the cheaper price, simple setup, and low temperature. Pure and cobalt-doped (0 – 3mol%) zinc oxide (ZnO) nanoparticles were synthesized via a chemical co-precipitation method. For the synthesis of pure ZnO, zinc acetate dihydrate was dissolved in 100 mL of double-distilled water, while a separate solution of potassium hydroxide (KOH) was prepared in 100 mL of double-distilled water. The two solutions were combined under continuous magnetic stirring at room temperature for 2 h to form a precipitate.

For the synthesis of Co-doped ZnO nanoparticles, stoichiometric amounts of zinc acetate dihydrate and cobalt acetate tetrahydrate were dissolved in 100 mL of double-distilled water, and a separate solution of KOH was prepared in 100 mL of methanol. The two solutions were mixed under constant magnetic stirring at room temperature for 2 h. In both cases, the resulting precipitates were isolated by filtration, washed thoroughly with distilled water and ethanol to eliminate impurities, and air-dried at 150 °C. Finally, the dried precursors were annealed in air at 400 °C for 8 h to yield pure and Co-doped ZnO nanoparticles.
The structural properties and crystal phase of the pure and Co-doped ZnO nanoparticles were analysed by X-ray diffraction (XRD) using a Rigaku diffractometer. Additionally, optical absorption spectra were recorded in the wavelength range of 200–800 nm using UV-Vis spectrophotometer.

III. RESULTS AND DISCUSSION

3.1 Microstructural analysis

Fig. 1 shows the XRD patterns of the pure, 1% and 3% Co-doped ZnO nanoparticles. The observed peaks are indexed to the hexagonal (wurtzite) structure of ZnO in well matched with JCPDS file no. 79 - 0207. the 2q peaks observed at 2θ = 31.07, 34.22, 36.14, 47.44, 56.66, 62.76. and 72.57^0 corresponding to crystal planes (100), (002), (101), (102), (110), (103) and (200) respectively. No any extra peaks were detected due to the presence of any secondary phases.

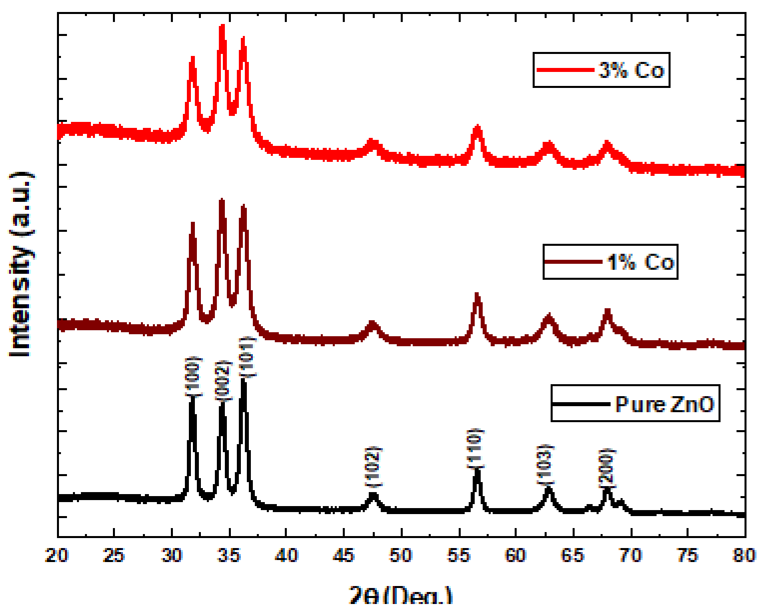

Fig. 1. X-ray diffraction patterns of undoped and Co-doped ZnO nanoparticles.

The lattice constants and other parameters are determined by using the XRD patterns and listed in the table 1. The lattice constants "a" and "c" showed slight decrease upon Co doping suggesting the successfully incorporation of Co into the ZnO lattice. Also, the cell volume of the ZnO was slight reductions after Co-doping because of ionic radii of Co^{2+} ions (0.58Å) has smaller than that of Zn^{2+} ions (0.65Å) [14, 15].

The crystallite sizes of all samples were calculated via Scherrrer's equation. The Scherrer's equation relates the crystallite size (D), to the FWHM (b), wavelength () and Bragg's angle () [16] as follows:

$$D = \frac{k\lambda}{\beta cos\theta} - - - - - (1)$$

The calculated crystallite sizes value is presented in table 1. The crystallite size of ZnO is decrease with

© NOV 2025 | IRE Journals | Volume 9 Issue 5 | ISSN: 2456-8880
DOI: https://doi.org/10.64388/IREV9I5-1722675

increase Co doping concentration. This may be attributed due to the small grain growth rate of ZnO sample as compared to Co-doped ZnO samples. Form this results, it is clear that prepared samples are in nano-sized suggesting that the samples have nanostructures [17, 18].

Table 1. Microstructural parameters of Co doped ZnO nanoparticles.

Samples Co doping	Lattice constants (Å)		Volume (V) (Å)^3	D (nm)
	a	c		
ZnO	3.2488	5.2118	47.6393	13.14
1%	3.2483	5.2118	47.6223	14.51
3%	3.2471	5.2135	47.6041	10.07

3.2 Optical Analysis

Optical analysis of the pure and Co-doped ZnO samples was conducted using a UV-Vis spectrophotometer (JASCO-7310) over the 200–1100 nm wavelength range (Fig. 2). As the Co doping concentration increased (Fig. 2), the absorption edge shifted towards longer wavelengths (redshift. This enhanced absorbance in the visible region is attributed to an increase in structural defect states within the forbidden bandgap. The relationship between the absorption coefficient (α) and photon energy ($h\nu$) for direct transitions are expressed by Tauc's relation:

$$\alpha h\nu = B(h\nu - E_g)^{1/2} - - - - - (2)$$

Where B is a material constant and E_g is the optical bandgap energy. Extrapolating the linear region of the $(\alpha h\nu)^2$ versus $h\nu$ Tauc's plots (Fig. 3a-c) revealed a systematic decrease in E_g with increasing Co dopant concentration (Fig. 3). This bandgap narrowing is primarily governed by s-d and p-d exchange interactions between the localized d-electrons of Co^{2+} ions and the s-band electrons of the host ZnO lattice, which can be described via second-order perturbation theory [19, 20]. This results confirming that the synthesized Co-doped ZnO nanoparticles are highly promising candidates for optoelectronic device applications.

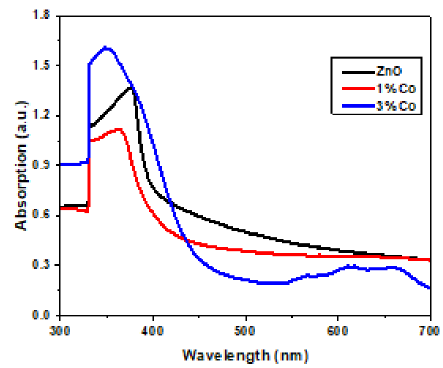

Fig. 2. Absorption spectra of undoped and Co-doped CuO nanoparticles.

© NOV 2025 | IRE Journals | Volume 9 Issue 5 | ISSN: 2456-8880
DOI: https://doi.org/10.64388/IREV9I5-1722675

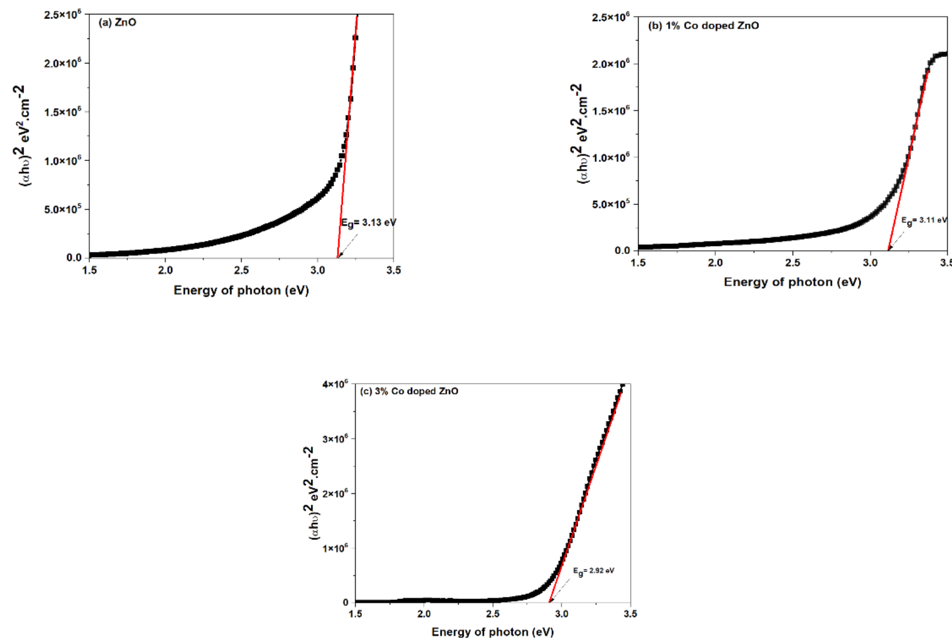

Fig. 3. Tauc's plots of undoped and Co-doped CuO nanoparticles.

IV. CONCLUSION

In summary, optoelectronics device based on Co-doped ZnO nanoparticles were successfully fabricated using the co-precipitation technique. X-ray diffraction analysis revealed a systematic reduction in both the lattice constants and unit cell volume with increasing Co content. Optical characterization demonstrated an enhanced absorbance in the visible region, accompanied by a bandgap narrowing from 3.13 eV to 2.92 eV, highlighting the suitability of nanoparticles for optoelectronic device applications.

V. REFERENCES

[1] Lu, F., Zhang, H., & Huang, X. (2022). Trends and emerging technologies for the development of electric vehicles. Energies, 15(17), 6271. https://doi.org/10.3390/en15176271

[2] Mejail, M., et al. (2025). The evolution of telecommunications: Analog to digital. Journal of Progress in Electronics and Communication Engineering, 2(1), 16–26.

[3] Baig, N., Kammakakam, I., & Falath, W. (2021). Nanomaterials: A review of synthesis methods, properties, recent progress, and challenges. Materials Advances, 2(6), 1821–1871. https://doi.org/10.1039/D0MA00807A.

[4] Roduner, E. (2006). Size matters: Why nanomaterials are different. Chemical Society Reviews, 35(6), 583–592. https://doi.org/10.1039/B502142C.

[5] Tiwari, J. N., Tiwari, R. N., & Kim, K. S. (2012). Zero-dimensional, one-dimensional, two-dimensional, and three-dimensional nanostructured materials for advanced energy utilization. Progress in Materials Science, 57(4), 724–803. https://doi.org/10.1016/j.pmatsci.2011.08.003.

[6] Dey, A. (2018). Semiconductor metal oxide gas sensors: A review. Materials Science and Engineering: B, 229, 206–217. https://doi.org/10.1016/j.mseb.2017.12.036.

[7] Miller, D. R., Akbar, S. A., & Morris, P. A. (2014). Nanoscale metal oxide-based heterojunctions for gas sensing: A review. Sensors and Actuators B: Chemical, 204, 250–272. https://doi.org/10.1016/j.snb.2014.07.074.

[8] Fine, G. F., Cavanagh, L. M., Afonja, A., & Binions, R. (2010). Metal oxide semi-conductor gas sensors in environmental monitoring.

Sensors, 10(6), 5469–5502. https://doi.org/10.3390/s100605469.

[9] Weldegebrieal, G. K. (2020). Synthesis method, antibacterial and photocatalytic activity of ZnO nanoparticles for biological applications: A review. Journal of Environmental Chemical Engineering, 8(4), 103933. https://doi.org/10.1016/j.jece.2020.103933

[10] Theerthagiri, J., Senthil, R. A., Priya, A., Madhavan, J., RJ, A. M., & Ashokkumar, M. (2019). Synthesis and characterization of zinc oxide nanostructures for photocatalytic degradation of organic pollutants: A review. Beilstein Journal of Nanotechnology, 10, 1740–1764. https://doi.org/10.3762/bjnano.10.169.

[11] Dey, A. (2018). Semiconductor metal oxide gas sensors: A review. Materials Science and Engineering: B, 229, 206–217. https://doi.org/10.1016/j.mseb.2017.12.036.

[12] Kolelyana, M., & Look, D. C. (2019). ZnO as a functional material, a review. Crystals, 9(10), 505. https://doi.org/10.3390/cryst9100505.

[13] Vijayalakshmi, S., & Venkataraj, S. (2013). Effect of metal doping on structural, optical, and electrical properties of ZnO thin films. Journal of Materials Science: Materials in Electronics, 24(8), 2845–2852.

[14] Bousslama, W., Elhouichet, H., & Ferid, M. (2017). Effect of cobalt doping on structural, optical, and magnetic properties of ZnO nanoparticles synthesized by sol-gel route. Journal of Materials Science: Materials in Electronics, 28(8), 6069–6078. https://doi.org/10.1007/s10854-016-6283-7

[15] Özgür, Ü., Alivov, Y. I., Liu, C., Teke, A., Reshchikov, M. A., Doğan, S., Avrutin, V., Cho, S.-J., & Morkoç, H. (2005). A comprehensive review of ZnO materials and devices. Journal of Applied Physics, 98(4), 041301. https://doi.org/10.1063/1.1992666

[16] Rabiei, M., Palevicius, A., Monshi, A., Nasiri, S., Vilkauskas, A., & Janusas, G. (2020). Comparing methods for calculating nano crystal size of natural hydroxyapatite using X-ray diffraction. Nanomaterials, 10(9), 1627. https://doi.org/10.3390/nano10091627.

[17] Marinov, G., Georgieva, B., Vasileva, M., & Babeva, T. (2023). Study of structure, morphology and optical properties of cobalt-doped and Co/Al-co-doped ZnO thin films deposited by electrospray method. Applied Sciences, 13(17), 9611. https://doi.org/10.3390/app13179611.

[18] Potera, P., Virt, I. S., & Cieniek, B. (2023). Structure and optical properties of transparent cobalt-doped ZnO thin layers. Applied Sciences, 13(4), 2701. https://doi.org/10.3390/app13042701.

[19] Bousslama, W., Elhouichet, H., & Ferid, M. (2017). Effect of cobalt doping on structural, optical, and magnetic properties of ZnO nanoparticles synthesized by sol-gel route. Journal of Materials Science: Materials in Electronics, 28(8), 6069–6078. https://doi.org/10.1007/s10854-016-6283-7

[20] Yüksekkaya, M. E., Aksu, S., & Erdem, F. B. (2021). Investigation of structural, optical bandgap narrowing, and s-d, p-d exchange interactions in transition metal-doped ZnO thin films. Physica B: Condensed Matter, 602, 412552. https://doi.org/10.1016/j.physb.2020.412552